



# Ultrastructure and in-situ chemical characterization of intracellular granules of embryo-like fossils from the early Ediacaran Weng'an biota

Weichen Sun<sup>1,2,3</sup> · Zongjun Yin<sup>1,2,7</sup> · Pengju Liu<sup>4</sup> · Philip C. J. Donoghue<sup>5</sup> · Jinhua Li<sup>6</sup> · Maoyan Zhu<sup>1,2,7</sup>

Received: 19 April 2021 / Accepted: 22 November 2021  
© Paläontologische Gesellschaft 2021

## Abstract

Embryo-like fossils from the early Ediacaran Weng'an biota provide a window of exceptional fossil preservation onto the period of life history in which molecular clocks estimate the fundamental animal lineages to have diverged. However, their diversity and biological affinities have proven controversial, because they are morphologically simple and, consequently, their interpretation lacks phylogenetic constraint. The subcellular structures preserved in these embryo-like fossils might help to understand their cytology, biology, and diversity, but the potential of these structures has not been fully realized, because detailed microscale physical and chemical investigations are lacking. Here, to remedy this deficiency, we performed a comprehensive study to characterize their micro- and ultra-structures as well as in-situ chemical components. Our results reveal three types of subcellular structure that differ in size, shape, and mineral components: (1) relatively small and spheroidal granules in embryo-like fossils with equal cell division pattern; (2) relatively large, spheroidal, or polygonal granules in embryo-like fossils with unequal and asynchronous cell division pattern; and (3) irregular multi-layered rim-bounded granules in embryo-like fossils with unequal and asynchronous cell division pattern. We propose that the three types may be rationalized to a single taphonomic pathway of preferential mineralization of the cell cytoplasm, preserving an external mould of subcellular granules. We followed the previous interpretation that the spheroidal and polygonal granules should be fossilized lipid droplets or yolk platelets. The distinction between these subcellular structures are largely the result of postmortem degradation processes such as autolysis. The widely preserved lipid droplets or yolk platelets within these Ediacaran embryo-like fossils are compatible with the interpretation of large yolky embryos with maternal nourishment and direct development.

**Keywords** Ediacaran · Weng'an biota · *Megasphaera* · Subcellular structure · Taphonomy

## Introduction

Fossilized subcellular structures including nuclei and other organelles are key characteristics in interpreting the fossil record of early eukaryotes (Pang et al. 2013; Yin et al. 2017;

Handling Editor: Joachim Reitner.

✉ Zongjun Yin  
zjyin@nigpas.ac.cn

<sup>1</sup> State Key Laboratory of Palaeobiology and Stratigraphy, Nanjing Institute of Geology and Palaeontology, Chinese Academy of Sciences, Nanjing 210008, China

<sup>2</sup> Center for Excellence in Life and Palaeoenvironment, Chinese Academy of Sciences, Nanjing 210008, China

<sup>3</sup> University of Science and Technology of China, Hefei 230026, China

<sup>4</sup> Institute of Geology, Chinese Academy of Geological Sciences, Beijing 100043, China

<sup>5</sup> School of Earth Sciences, Life Sciences Building, University of Bristol, Tyndall Avenue, Bristol BS8 1TQ, UK

<sup>6</sup> Key Laboratory of Earth and Planetary Physics, Institute of Geology and Geophysics, Innovation Academy for Earth Science, Chinese Academy of Sciences, Beijing 100029, China

<sup>7</sup> College of Earth and Planetary Sciences, University of Chinese Academy of Sciences, Beijing 100049, China

Sun et al. 2020). However, a few studies have focused on these tiny structures, because their fossilization potential is thought to be low (Baillieu 2021; Carlisle et al. 2021). The early Ediacaran Weng'an Biota from the Doushantuo Formation, Guizhou Province, southwestern China has yielded abundant phosphatized embryo-like fossils with exceptional preservation of subcellular structures, providing a unique window to exploring the evolution history of multicellular eukaryotes 609 million years ago (Xiao et al. 2014a; Cunningham et al. 2017; Bottjer et al. 2020).

The Ediacaran Weng'an embryo-like fossils (embryoïdes) have attracted considerable attention, because they were initially interpreted as embryos of early animals (Xiao et al. 1998, 2007a; Xiao and Knoll 1999, 2000; Chen et al. 2000, 2006, 2009a, 2009b; Yin et al. 2007, 2013, 2016) and later as unicellular relatives of metazoans (i.e., non-metazoan holozoans) (Huldtgren et al. 2011) or stem-metazoans (Hagadorn et al. 2006; Chen et al. 2014). The Weng'an embryoïdes have also been interpreted as giant sulfur bacteria (Bailey et al. 2007), but this is at least one hypothesis that can be rejected based on comparative taphonomy and biology (Xiao et al. 2007b; Yin et al. 2007; Cunningham et al. 2012b). Discriminating among the remaining hypotheses is challenging because of the simple morphology of the embryoïdes, comprised as they are as simple geometric arrangements of cells. Nevertheless, recent studies have converged on a holozoan affinity based on new data on their development biology (Yin et al. 2019, 2020). However, their biodiversity and precise phylogenetic affinity within Holozoa remain unresolved.

Here, we focus on the subcellular structures commonly preserved in the Weng'an embryoïdes in attempt to further constrain their biology. The significance of these structures has been unclear, since they were first reported 15 years ago (Hagadorn et al. 2006), but micro- and even nano-scale physical and chemical characterization of these subcellular structures might be helpful to understanding not only their preservation mechanisms but also the cytology and biology of the Weng'an embryoïdes.

Two main types of subcellular structure have been reported from the Weng'an embryoïdes. Large intracellular structures have spheroidal-to-reniform morphologies, exhibiting consistency in the number (generally one per cell, or sometimes two in cells undergoing division) and relative size (relative to the volume of the cell). Though they have previously been interpreted as degraded remains or diagenetic structures (Schiffbauer et al. 2012; Pang et al. 2013), the large intracellular structures have now been confirmed as the fossilized remains of nuclei based on diverse evidence (Hagadorn et al. 2006; Chen et al. 2009b; Huldtgren et al. 2011; Yin et al. 2017; Sun et al. 2020; Carlisle et al. 2021).

Alternatively, small intracellular granules exhibit various shapes (spherical, oval or polygonal) and sizes (10 µm to about 50 µm) (Hagadorn et al. 2006; Chen et al. 2009a).

They usually occur within cells in large numbers (Hagadorn et al. 2006; Chen et al. 2009a). Previous studies have interpreted these structures as membrane-bound cytoplasmic vesicles, coated yolk granules, or lipid droplets in cleaving blastomeres of animal embryos based merely on similar size and shape (Hagadorn et al. 2006). However, the variation in the nature and significance of the subcellular granules and their preservation modes remain unclear. While they have been interpreted as yolk granules or lipid vesicles, reflecting maternal investment and direct development (Hagadorn et al. 2006), lipid droplets also coalesce postmortem as a product of autolysis (Raff et al. 2006, 2008; Gostling et al. 2008). Furthermore, comparable structures form as clotted fabric, as consequence of diagenetic mineralization after decay of the original biological tissues (Hagadorn et al. 2006) and, as such, they are uninformative of the biology of the original organism. Thus, in an attempt to discriminate between biological, taphonomic, and geological interpretations of these small intracellular structures, we characterized their structure and in-situ elemental components in micro- and even nano-scale.

## Materials and methods

Specimens in this study were collected from the Upper Phosphate Member (or Weng'an Phosphate Member) of the Ediacaran Doushantuo Formation (635–551 Ma) at 54 Quarry in the Weng'an phosphate mining area in Guizhou Province, Southwestern China (Xiao et al. 2014a; Cunningham et al. 2017; Bottjer et al. 2020). Rock samples of grey dolomitic phosphorite were dissolved in ca. 10% acetic acid and then separated from the resulting residue by manual picking under stereomicroscope. Morphological and structural observations were carried out by a combination of X-ray microscopic tomography (micro-CT), scanning electron microscopy (SEM), focused ion beam- scanning electron microscopy (FIB-SEM), and transmission electron microscopy (TEM). Element analysis was performed using energy-dispersive X-ray spectroscopy (EDS) which is coupled with a field emission SEM.

## Taxonomy

In previous studies, the Weng'an embryoïdes are described under various genus and species name include *Megasphaera*, *Parapandorina*, *Megaclonophycus*, and *Tianzhushania* because of the different taxonomic interpretations (Xiao and Knoll 2000; Huldtgren et al. 2011; Cunningham et al. 2012a; Chen et al. 2014; Xiao et al. 2014a, b). While Xiao and Knoll have argued that *Megasphaera* is a form taxon, likely encompassing many biological species (Xiao and Knoll 2000), the majority of studies of the Weng'an biota

have treated it as a coherent biological taxon (Bailey et al. 2007; Huldtgren et al. 2011; Chen et al. 2014; Zhang and Pratt 2014) and, indeed, many researchers have interpreted the diverse components of the Weng'an Biota as stages in the life cycle of just one or a smaller number of taxa (Xiao et al. 2007a; Huldtgren et al. 2011; Zhang and Pratt 2014). Nevertheless, irrespective of their taxonomic status, fossils attributable to all of these genera exhibit similarities in the nature and variation of their subcellular structure. As such, we describe them as one assemblage that we attribute to *Megasphaera*.

### X-ray microscopic tomography

We conducted high-resolution microtomographic analyses using a Carl Zeiss Xradia 520 Versa X-ray tomographic microscope at the Micro-CT Lab of the Nanjing Institute of Geology and Palaeontology, Chinese Academy of Sciences (NIGPAS). To achieve high contrast, we used an operating voltage of 50 kV and power of 4 W of the X-ray tube. Depending on the size of the specimens, a charge-coupled device (CCD)-based optical objective (4×) was applied, yielding isotropic voxel dimensions of 0.8–1.3 μm. To reduce beam-hardening artifacts, two X-ray thin filters (LE1 and LE2) were used. For each scan, 3601 equi-angular projections over 360° were obtained. Volume data were processed using VGStudio Max (3.0 version). The tomographic data are freely available from the University of Bristol Research Data Repository at <https://doi.org/10.5523/bris.1smpsrc4bipqi25rytwr9xgujc> and <https://doi.org/10.5523/bris.pxup7vdmg25r2sl3kr00y5cu6>.

### EDS-SEM

Based on the tomographic data, specimens with well-preserved subcellular structures were selected for further preparation at the Institute of Vertebrate Paleontology and Paleoanthropology, Chinese Academy of Sciences (IVPPCAS). Specimens were first embedded within light-cured resins (TECHNOVIT 7200VLC), and then cut using diamond-encrusted wire saw (EXAKT 300CP, 0.1 mm thick). The slices were then polished by diamond polishing agent (1 μm in diameter) until the subcellular structures were exposed. The cytoplasmic granules were observed using EDS-coupled field emission scanning electron microscope TESCAN MAIA3 at NIGPAS. Both secondary electron and backscattered electron detectors were used for SEM imaging with accelerating voltages ranging from 5 to 15 kV. EDS mapping was performed at the optimal beam condition (5–10 kV).

### FIB-SEM and TEM

The FIB cutting was conducted with a Zeiss Auriga Compact dual beam instrument equipped with an Omniprobe AutoProbe 200 micromanipulator at the Institute of Geology and Geophysics, Chinese Academy of Sciences (IGGCAS). Final thinning and polishing for ultrathin sections were conducted using an ion beam with an accelerating voltage of 5 kV and beam currents of 50 pA to 2 nA. The ultrathin sections were prepared to ~100 nm thickness. TEM bright-field imaging, selected area electron diffraction (SAED), and high-resolution transmission electron microscopy (HRTEM) imaging were carried out using a JEOL JEM-2100 TEM operated at 200 kV.

## Results

Well-preserved *Megasphaera* with intracellular granules were selected from among a large number of Weng'an embryo-like fossils with the help of high-resolution X-ray microscopic tomography. Intracellular granules are easily identified based on differences in X-ray attenuation relative to the surrounding matrix. On this basis, we were able to organize the variation seen into two classes of specimens and we describe them as such.

### X-ray microscopic tomography exhibits diverse shapes, sizes, and distribution of granules

In the first group of specimens, abundant intracellular granules are preserved in association with a larger nucleus (Fig. 1a–d, Fig. 2a–f). The intracellular granules are mainly spheroidal or ovoid with a maximum diameter of 5–30 μm (Figs. 1d, 2a–f). The margin of the granules is defined by a mineral phase comprising a rim with high X-ray attenuation and an inner body exhibiting relatively low X-ray attenuation (Figs. 1a–d, 2a–f). For example, Fig. 1a–d exhibits an incomplete 16-celled *Megasphaera* with equal and synchronous cell division. It possesses five complete cells and three broken cells. In each cell, there is a large nucleus with diameter around 200 μm and many granules with spherical or oval shape (Fig. 1a–c).

In the second group of specimens, the intracellular granules are more irregular, exhibiting spheroidal, ovoid, or polyhedral morphologies, and they are relatively larger, approximately 30–40 μm in maximum diameter (Fig. 3). These granules are invariably associated with specimens that exhibit unequal and asynchronous cell division and every cell in every such specimen that we examined was filled with these granules (Fig. 3). Interestingly, however, none of these cells preserved a nucleus. Nearly all of the polyhedral granules were preserved in a low X-ray attenuating

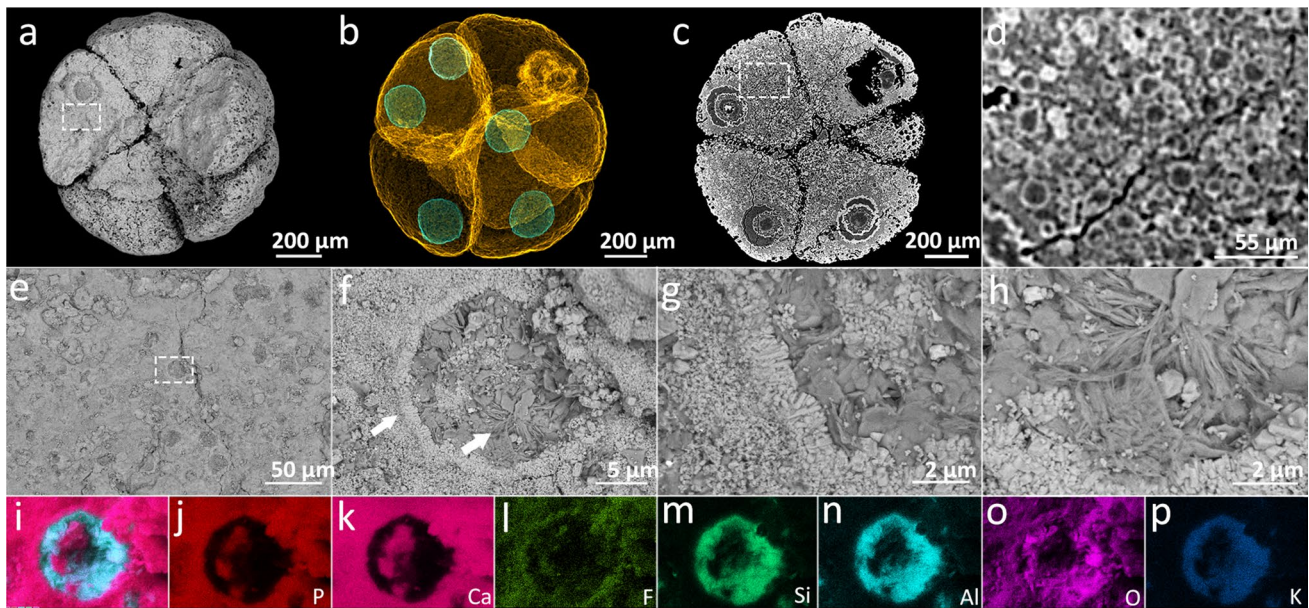


**Fig. 1** Subcellular structures in a 16-celled specimen of *Megasphaera* from the Ediacaran Weng'an Biota. **a** SEM image showing the fracture surface. **b** Micro-CT rendering with transparent mode of (**a**). **c** Tomographic virtual section showing subcellular structures. **d**, **e**

Close-up views of the framed areas in (**c**) and (**a**), respectively. **f** A close-up view of a granule marked in (**e**). **g**, **h** Magnified views showing mineral detail of rim and inner body of the granule in (**f**). **i** Composition of (**j**–**p**). **j**–**p** EDS elemental mapping of the granule in (**f**)

mineral phase but well defined by a rim with higher (Fig. 3q, r) or lower X-ray attenuation (Fig. 3s, t). One 2-celled specimen preserved granules with an irregular multi-layered rim (Fig. 6a–f).

### EDS-SEM reveals the mineral composition of the granules

Our data suggest that the cell cytoplasm is preserved as apatite, while the intracellular granules show different mineral composition. Type One preserves intracellular granules as an apatite rim and clay inner body. For example, the intracellular granules of specimen in Fig. 1 exhibit a rim which is composed of oriented columnar crystals that are relatively larger than the microcrystalline in cytoplasmic matrix (Fig. 1e–g), while the minerals within the inner body regions seem to be fibrous to platy (Fig. 1f–h). EDS elemental mapping indicates that the higher attenuation mineral phases have a higher relative concentration of P, Ca and F, while the lower attenuation mineral phases have a higher relative concentration of Si, Al, O, and K (Fig. 1i–p). When combining the two lines of evidence on the spatial distribution of elements and crystal habits, we interpret the high and low attenuation mineral phases as apatite and clay, respectively. Type Two preserves the intracellular granules as a homogenous apatite rim and inner body. This type of mineral composition occurs in specimens of *Megasphaera* that exhibit both equal and unequal cell division. For example, the granules preserved in specimens with equal cell division

exhibit a ca. 2 µm-thick rim which exhibits lower attenuation than the minerals of the surrounding matrix (Fig. 2a–c). These granules are also spheroidal or ovoid but smaller, with a maximum diameter ranging 10–20 µm. EDS elemental mapping indicates that both the rim and inner body were preserved as apatite (Fig. 2). The granules preserved in specimens with unequal and asynchronous cell division also show the same mineral composition (Figs. 3, 4). Nearly all of the polyhedral granules were preserved in a low X-ray attenuating mineral phase but remain well defined by a rim with higher (Fig. 3q, r) or lower X-ray attenuation (Fig. 3s, t) than the surrounding matrix. EDS elemental mapping shows that the chemical composition of the entire specimen is homogeneous, with high relative concentration of Ca, P, and O (Fig. 4). These observations suggest that the contrast between the rim and the inner body results from crystalline textural and trace chemical variation rather than a fundamental compositional difference. Type Three preserves the granules as rim-bounded void spaces that may never have been mineralized or else may have been filled with calcite or dolomite that was dissolved by the acetic acid used to recover the fossils (Fig. 2b, arrows).

### FIB-SEM and TEM characterize mineral phases of the granule rim

To understand the preservation mode of the granules, we applied FIB-SEM and TEM to reveal the mineral phases of the rim and inner body (Fig. 5). We made an ultrathin

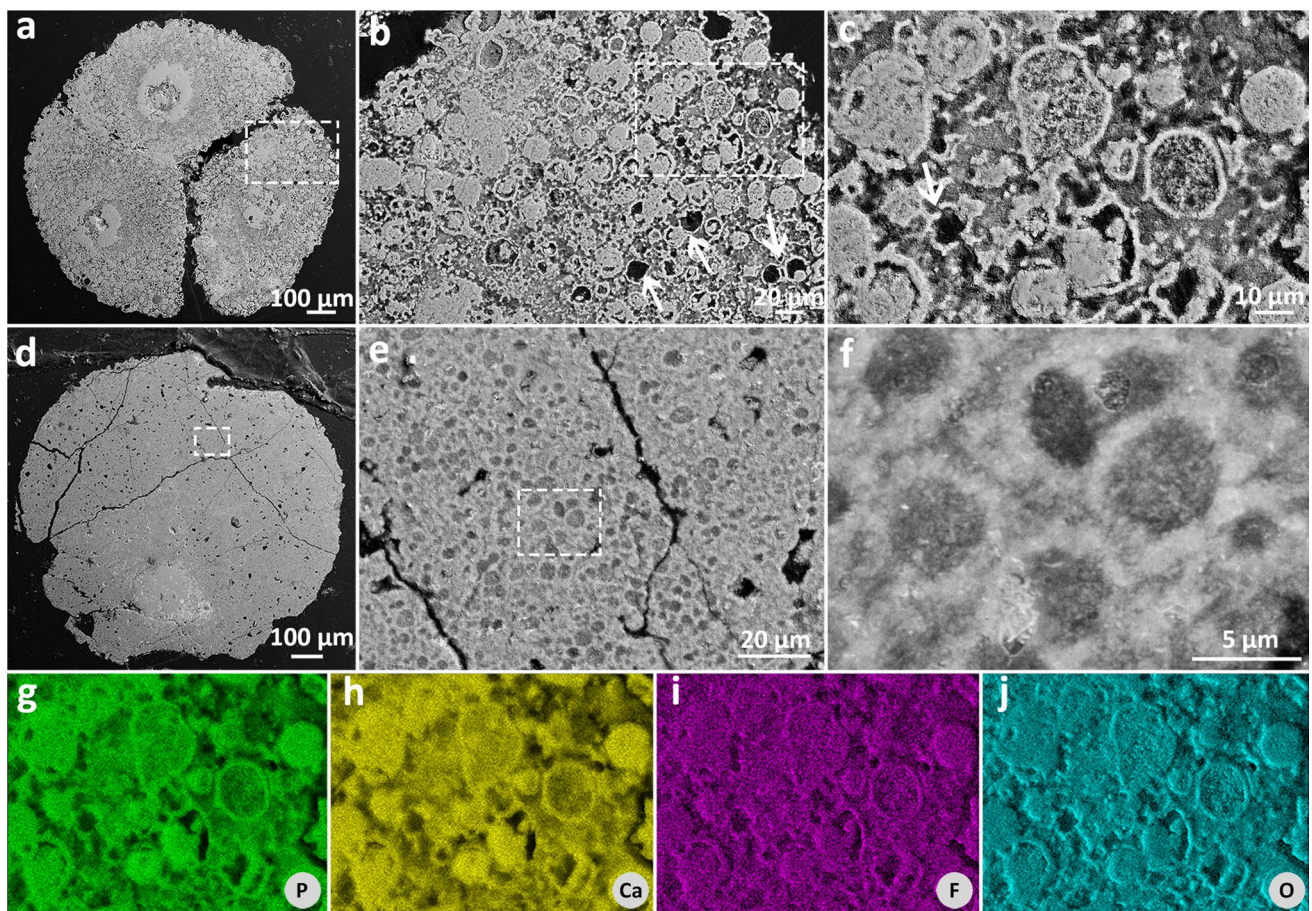


**Fig. 2** Subcellular granules of *Megasphaera* from the Ediacaran Weng'an Biota. **a, d** Two physical cross sections showing subcellular granules. **b, e** Close-up views of framed areas in (**a, d**), respectively.

(**c, f**) Magnifications of the two framed areas in (**b, e**), respectively, showing detail of granules (**g–j**) EDS elemental mapping of the granules in (**c**)

section (about 10  $\mu\text{m}$  long, 2  $\mu\text{m}$  wide, 100 nm thick) across the boundaries of two granules using FIB (Fig. 5d, e), and then observed it using TEM (Fig. 5e–i). The TEM images show that the two rims at the margin of granules consist of oriented submicron to tens of nanometer-sized columnar apatite crystals that are orientated perpendicular to the surface of inner body (Fig. 5e–g, i, j). In contrast, the inner body and surrounding matrix are characterized by randomly oriented submicron to nanometer scale crystals of apatite (Fig. 5f–h). We also applied FIB-SEM and TEM to the irregular granule which was enveloped by a multi-layered rim (Fig. 6). High magnification of the granule rims reveals two layers of oriented columnar apatite crystals that are orientated perpendicular to the surface of the inner body (Fig. 6d–i). In addition, the ultrastructure of the membrane-like rim is different from the rims of other granules described above (Fig. 5). The bi-layered membrane-like rim is approximately 1  $\mu\text{m}$  thick, each layer less than 500 nm in thickness (Fig. 6f–i). In contrast, the rims of the other granules are always single-layered and often more than 2  $\mu\text{m}$

in thickness. Furthermore, the size of the apatite crystals preserving the bi-layered granule rim is smaller than that preserving the rims of other granules.

## Discussion

The Weng'an embryo-like fossils preserve abundant subcellular structures with high fidelity, providing a unique window through which to explore the cytology and biology of these early Ediacaran multicellular eukaryotes. Previous studies had mainly focused on the nuclei (Hagadorn et al. 2006; Hultgren et al. 2011; Schiffbauer et al. 2012; Yin et al. 2017; Sun et al. 2020), while there have been few studies on the smaller but more numerous intracellular granules (Hagadorn et al. 2006; Raff et al. 2008). To understand the nature of these small granules, we characterized their morphologies, structure, and in-situ chemical components in micro- to nano-scale using a combination of microscopy and spectroscopy techniques. Our results indicate that the

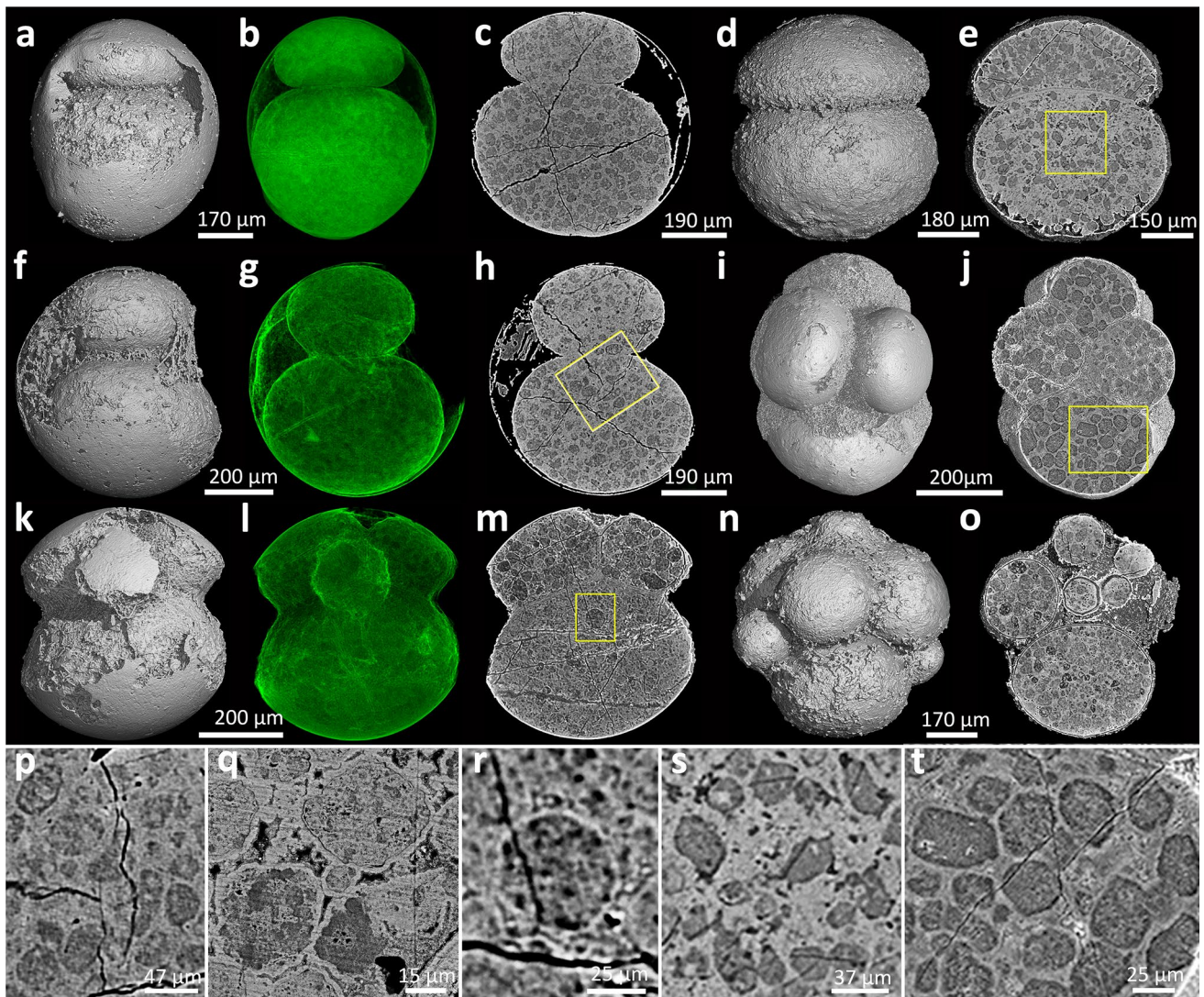


**Fig. 3** Six specimens of *Megasphaera* from the Ediacaran Weng'an Biota. **a, d, f, i, k, n** Surface renderings. **b, g, l** Renderings in transparent mode of (**a, f, k**) respectively. **c, e, h, j, m, o** Virtual sec-

tions of (**a, d, f, i, k, n**), respectively, showing internal structures. **p–t** Close-up views of framed areas in (**e, h, g, m**), showing detail of granules

subcellular granules are not uniform in nature, but exhibit variation in size, shape, mineralogy, and presence or absence of an inner body.

### Distinguishing geology and biology

All of the granules that we observed exhibit rims composed of radially arranged apatite crystals that diverge centripetally (Fig. 1e–h) into the interior of granules. Locally, the inner surfaces bulge where clusters of crystals have grown longer than those around them. In some spaces, the lumen is mostly filled with mineral exhibiting the same X-ray attenuation profile, either as a massive mineralization or divided into local rosettes of centripetal mineralization (Figs. 2a–c; 3q). The lumen is otherwise occupied partially or fully with clay

mineral or void-filling apatite, or else the lumen is unfilled—either because it was never mineralized or because the dolomite or calcite void-filling mineralization has leached away by the acetic acid preparation to recover the fossils from the rock. The euhedral and polarized nature of the mineral phase comprising the rims and its common trace chemistry with the void-filling phases indicates that it does not reflect mineralization of an original biological matrix. However, the polarized nature of the centripetal growth reflects growth from a substrate that is no longer preserved. We interpret this substrate as the original biological feature preserved in the fossils and the mineralization associated with inner lumen as void-filling, regardless of the style of mineralization.

The remaining differences between the types of granules that we have described concern consistency in shape and

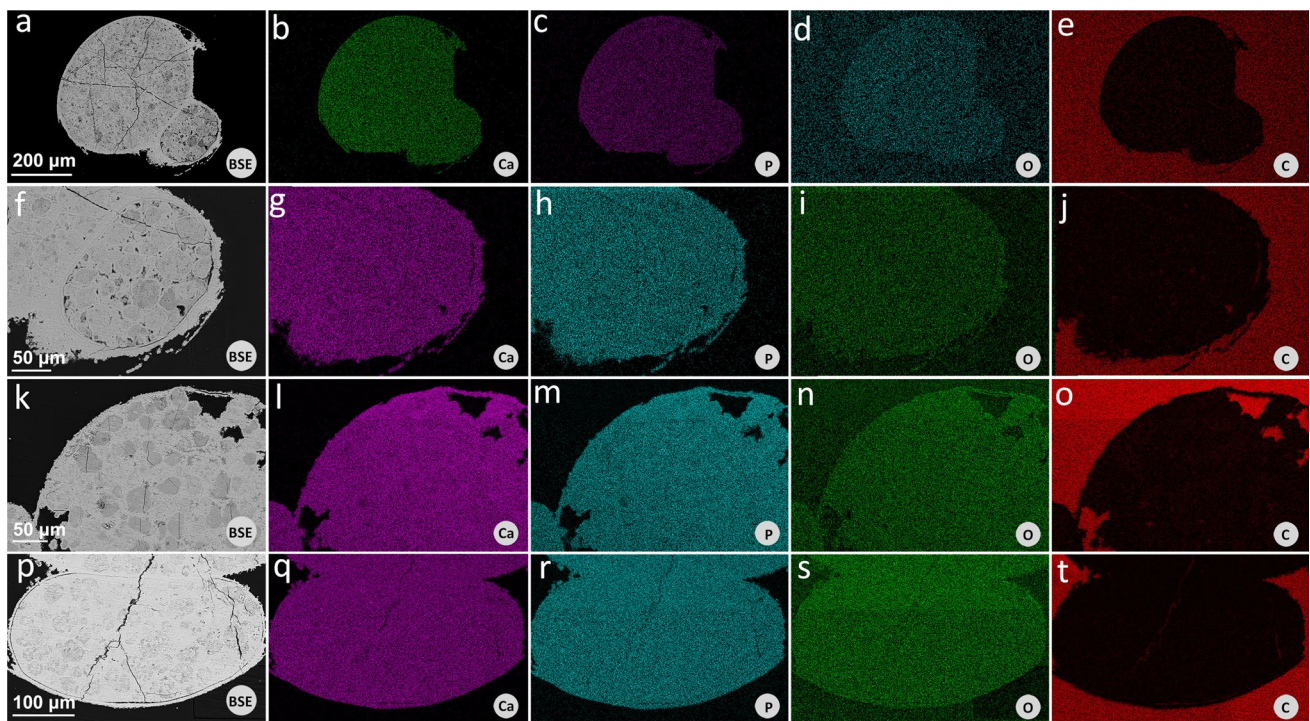


**Fig. 4** EDS elemental mapping of the specimens in Fig. 3. **a** A physical cross section of the specimen in Fig. 3k (BSE SEM image), with magnified detail displayed in **(f)**. **k** An enlarged view of a physical cross section of the specimen in Fig. 3d (BSE SEM image). **p** An

enlarged view of a physical cross section of the specimen in Fig. 3f. **b–e**, **g–j**, **l–o**, **q–t** EDS elemental mapping of the areas in **(a, f, k, p)**, respectively

size. The type (i) granule shows spheroidal shape. The polarized crystals of the rim grow from a substrate that is no longer preserved and the mineralized cytoplasmic matrix provides templates for them. The clay or apatite inner body represents the later void-filling (Figs. 1, 2). In this situation, the granules have enough time to degrade and preserved as relatively original shape.

The type (ii) granule shows spherical or polyhedral shape. They are larger than the first type and always filled up the host cells which looks more crowded (Figs. 3, 4, 5). In some areas of the specimen, the granule shows spherical shape (Fig. 3r). However, in most instances, they are close to each other and show polyhedral but not uniform shape (Fig. 3p–q, s–t). We speculate that the polyhedral shape is the result of space constraints during the growing of oriented crystals.

The type (iii) granule with irregular shape and multi-layered rim is also preserved in the same specimen (Fig. 6). The outline of this granule shows that plastic deformation indicates that it undergoes slight dehydration and contraction during postmortem degradation process, before it was fully permineralized. The two layers of oriented columnar apatite crystals are orientated perpendicular to the surface of the inner body. We propose two possibilities of the form of bi-layered rim: one is the granule has an original membrane which provided a template from which the apatite

crystals grew centripetally and centrifugally. In this case, the membrane was located at the boundary between the two layers, later decaying away. The other envisages the bi-layered rim as having form via multiple phases of later diagenetic mineral lining and coating. In either instance, the rims themselves do not represent original organic membrane structures.

The type (i) granule was first reported by Hagadorn et al. in 2006 and the type (ii) was first found by Chen et al. in (2009a, b). Hagadorn et al (2006) interpreted the granules as cytoplasmic nutrients such as yolk granules or lipid droplets. This interpretation was followed by the subsequent studies (Chen et al. 2009a). When comparing with subcellular structures of extant holozoan cells, these granules are much smaller than nuclei and much larger than any spherical or ovoid membrane-bounded organelles such as mitochondria and lysosomes. Some other organelles including Golgi apparatus and endoplasmic reticula are relatively larger, but they differ from these fossil granules in three-dimensional architecture and structure. Moreover, no organelles other than cytoplasmic nutrients such as yolk and lipid are present in such high abundance in holozoan cells. Therefore, given the size, shape, and abundance of these granules within cells, it is reasonable to interpret the type (i) granules as

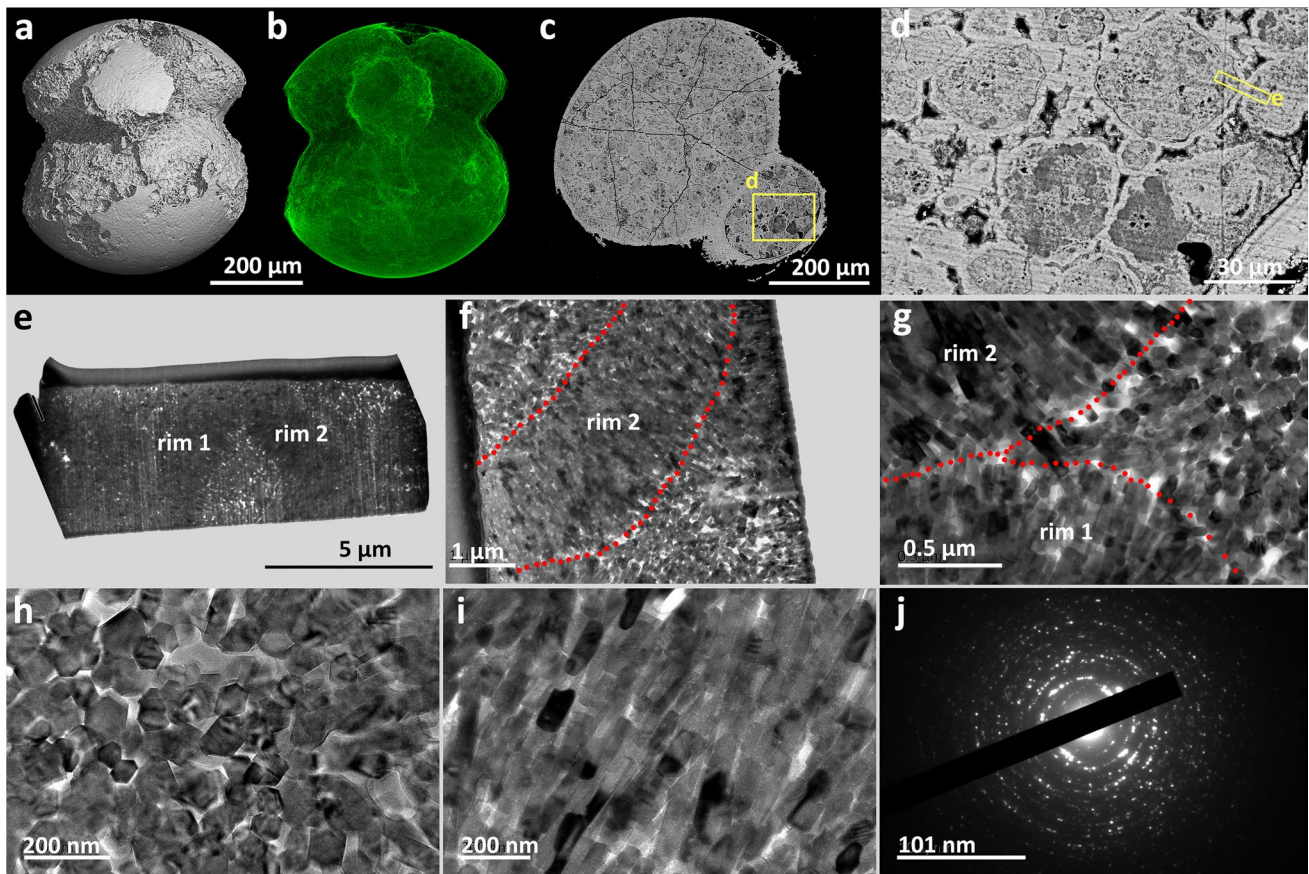


**Fig. 5** A *Megasphaera* specimen with subcellular granules from the Ediacaran Weng'an Biota. **a** Surface rendering of a 4-celled specimen in Fig. 3k. **b** Rendering with transparent mode of (a). **c** A physical cross section of (a) (BSE SEM image). **d** A close-up view of the framed area marked in (c), showing detail of granules. **e** Focused ion

beam-cut ultrathin section of the framed area marked in (d). **f–i** TEM images of the ultrathin section, showing minerals of rims and inner body of granules. **j** Selected area transmission electron diffraction pattern of apatite crystals in (i), reflecting the orientation of the crystals

nutrients; the type (ii) and (iii) may represent the postmortem remains of yolk granules or lipid droplets.

### Correlation between the granules and embryoids

These types of intracellular granule correlate with differences in the cell division patterns of the host specimens. For example, the type (i) granules are always preserved in specimens with equal cell division and there always has a nucleus in each host cell. While the type (ii) and (iii) granules are associated with specimens with unequal cell division. The six specimens with unequal cell division shown in this paper have different number of cells. Moreover, each specimen has the largest cell and each cell of them is preserved as complete and full ovoid shape. Therefore, we reject the diagenetic interpretation of unequal cell size. Together with the correlation between the granules and cell division mode, we suggest that these Weng'an embryo-like fossils do not belong to the same species, though they have long been assigned to one morphological species. Recent studies

on *Helicoforamina* and *Caveasphaera* also illustrated that the biodiversity of the Weng'an embryo-like fossils has been underestimated (Yin et al. 2019, 2020), but the diversity within the morphological genus *Megasphaera* remains indistinct.

### Comparison with the preservational pathway of nuclei

Type (i) granules tend to be preserved always in association together with cell nuclei. These cell nuclei are different in shape, presence or absence of an inner body, and chemistry of the associated mineralization (Hagadorn et al. 2006; Schiffbauer et al. 2012; Yin et al. 2017; Sun et al., 2020). Previous studies have confirmed that a single taphonomic pathway in which the cell cytoplasm is the first to mineralize soon after death, resulting in external moulds of the remaining cell volume (Yin et al. 2017; Sun et al. 2020). Experimental taphonomy of epidermal cells from the common onion demonstrates that nuclei are more decay resistant than

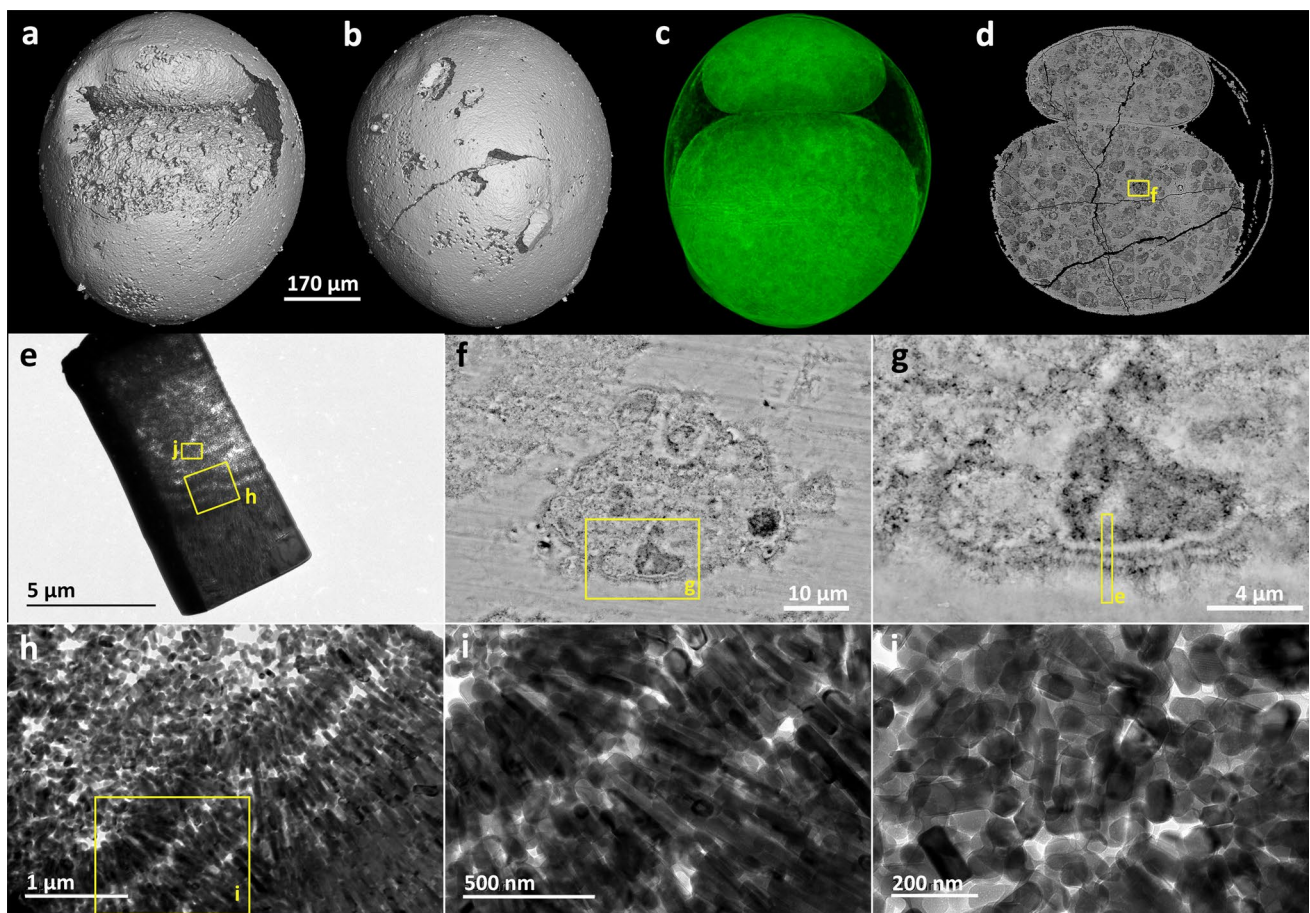


**Fig. 6** A *Megasphaera* specimen with subcellular granules from the Ediacaran Weng'an Biota. **a, b** Surface renderings of the same specimen in Fig. 3a. **c** Rendering with transparent mode of (a). **d** A physical cross section of (a). **e** A FIB-cut ultrathin section of the framed area in (g). **f, g** Close-up views of framed areas in (d, f) (BSE SEM

images), respectively, showing an irregular granule. **h, i** TEM images of areas marked in (e) and (h), showing three layers of oriented apatite crystals. **j** TEM images of area marked in (e), showing the minerals of inner body of granules

their host cells, making them available as substrates for mineralization on time scales compatible with exceptional fossil preservation (Sun et al. 2020). Type (i) granules preserved as spheroidal shape, clay or apatite inner body, and apatite rim. These features are consisted with the taphonomic pathway of nuclei. The cell cytoplasm mineralized selectively soon after death of the embryoids. Subsequently, the nuclei and yolk granules were preserved.

However, the type (ii) granules show polygonal shape which suggests that they have decayed, and type (iii) granules show irregular margins which suggest that they exhibit decay prior to mineral replication. Therefore, the type (ii) and (iii) indicate that these structures are probably preserved over a long period of time after the embryoid death and after some autolysis. We noticed that no large nuclei were preserved within the host cells for the type (ii) and (iii) granules so far. This phenomenon is likely a taphonomic bias, because these cells encountered greater postmortem degradation, as reflected in the two types of granules.

### Implications for understanding the developmental biology of *Megasphaera*

Attempts to understanding the level of evolution of early multicellular life in the fossil record have been stymied by the simplicity of the preserved aspects of organism structure. Therefore, the diversity and phylogenetic affinities of these Ediacaran Weng'an embryoids have long been debated. Though recent studies have attributed them into Holozoa with strong confidence and suggested that their biodiversity is probably much higher than previously thought (Yin et al. 2019, 2020), their precise biodiversity and phylogenetic affinity within Holozoa remain unresolved. More developmental biology information of these Weng'an embryoids would be critical to further constrain their precise diversity and affinity. The subcellular granules, widely interpreted as lipid droplets or yolk platelets, occurred in large numbers within the cells of *Megasphaera*, suggesting that at least some embryo-like fossils from the Weng'an Biota were

yolk-rich, reflecting maternal nourishment and direct development. Similar inferences have been made of the developmental biology of *Caveasphaera* (Yin et al. 2019).

## Conclusion

Subcellular granules inform on the cytology and developmental biology of the Weng'an embryo-like fossils, potentially informing on their diversity and affinity. In this study, we implemented physical and in-situ chemical characterization of the subcellular granules in micro- to nano-scale and identified at least three types of granules in the Weng'an *Megasphaera*: (i) spheroidal shape, clay or apatite inner body, and apatite rim; (ii) irregular or polyhedral shape, homogeneous apatite rim, and inner body; (iii) irregular shape, multi-layered apatite rim, and apatite inner body. We interpret the type (i) granules as maternal nutrients, while the type (ii) and (iii) may represent the postmortem products of yolk or lipids. Our observations suggest that the taphonomic pathway of type (i) granules is similar to that of large cell nuclei, while the type (ii) and (iii) granules encountered relatively longer degradation after death.

We discovered a correlation between the granule types and the cell division patterns of the fossils, i.e., type (i) granules only appear in equally and synchronously cleaving embryo-like fossils, while the type (ii) and (iii) granules appear in unequally and asynchronously cleaving embryos. This correlation could be interpreted as a taphonomic bias, but the underlying taphonomic mechanism remains unknown. We propose that the biodiversity within the morphological genus *Megasphaera* is probably higher than previously thought, not only because many *Megasphaera* specimens developed different types of ornamentations on the surface (Xiao and Knoll 2000; Yin and Zhu 2012), but also because they applied various cell division patterns. Abundant subcellular granules as maternal nutrients filling the fossil cells is compatible with the inference that some of these Ediacaran Weng'an embryo-like fossils were direct developers (Hagadorn et al. 2006).

**Acknowledgements** We would like to thank Suping Wu and Yan Fang from the Experimental Technologies Center of NIGPAS for their help in tomographic reconstruction and EDS elemental mapping. We also would like to thank Lixin Gu from the Electron Microscopy Laboratory of IGGCAS, Shukang Zhang from IVPP and Yanhong Pan from Nanjing University for their helps in sample preparation. This research is supported by Strategic Priority Research Program (B) of the Chinese Academy of Sciences (CAS) (XDB26000000), the National Natural Science Foundation of China (42022010, 41921002), CAS Interdisciplinary Innovation Team (JCTD-2020-18), and the Youth Innovation Promotion Association of the CAS. In addition, Zongjun Yin, Philip Donoghue and Maoyan Zhu were funded by Natural Environment Research Council (NERC) grant (NE/P013678/1), part of the Biosphere Evolution, Transitions and Resilience (BETR) programme, which is co-funded by the Natural Science Foundation of China (NSFC).

## References

- Bailey, J.V., S.B. Joye, K.M. Kalanetra, B.E. Flood, and F.A. Corsetti. 2007. Evidence of giant sulphur bacteria in Neoproterozoic phosphorites. *Nature* 445: 198–201.
- Bailleul, A.M. 2021. Fossilized cell nuclei are not that rare: review of the histological evidence in the Phanerozoic. *Earth-Science Reviews* 216: 103599.
- Bottjer, D.J., Z.J. Yin, F.C. Zhao, and M.Y. Zhu. 2020. Comparative taphonomy and phylogenetic signal of phosphatized Weng'an and Kuanchuanpu Biotas. *Precambrian Research* 349: 105408.
- Carlisle, E.M., M. Jobbins, V. Pankhania, J.A. Cunningham, and P.C.J. Donoghue. 2021. Experimental taphonomy of organelles and the fossil record of early eukaryote evolution. *Science Advances* 7: eabe9487.
- Chen, J.Y., P. Oliveri, C.W. Li, G.Q. Zhou, F. Gao, J.W. Hagadorn, K.J. Peterson, and E.H. Davidson. 2000. Precambrian animal diversity: putative phosphatized embryos from the Doushantuo formation of China. *Proceedings of the National Academy of Sciences of the United States of America* 97: 4457–4462.
- Chen, J.Y., D.J. Bottjer, E.H. Davidson, S.Q. Dornbos, X. Gao, Y.H. Yang, C.W. Li, G. Li, X.Q. Wang, D.C. Xian, H.J. Wu, Y.K. Hwu, and P. Tafforeau. 2006. Phosphatized polar lobe-forming embryos from the Precambrian of Southwest China. *Science* 312: 1644–1646.
- Chen, J.Y., D.J. Bottjer, E.H. Davidson, G. Li, F. Gao, R.A. Cameron, M.G. Hadfield, D.C. Xian, P. Tafforeau, Q.J. Jia, H. Sugiyama, and R. Tang. 2009a. Phase contrast synchrotron X-ray microtomography of Ediacaran (Doushantuo) metazoan microfossils: Phylogenetic diversity and evolutionary implications. *Precambrian Research* 173: 191–200.
- Chen, J.Y., D.J. Bottjer, G. Li, M.G. Hadfield, F. Gao, A.R. Cameron, C.Y. Zhang, D.C. Xian, P. Tafforeau, X. Liao, and Z.J. Yin. 2009b. Complex embryos displaying bilaterian characters from Precambrian Doushantuo phosphate deposits, Weng'an, Guizhou, China. *Proceedings of the National Academy of Sciences of the United States of America* 106: 19056–19060.
- Chen, L., S.H. Xiao, K. Pang, C.M. Zhou, and X.L. Yuan. 2014. Cell differentiation and germ-soma separation in Ediacaran animal embryo-like fossils. *Nature* 516: 238–241.
- Cunningham, J.A., C.W. Thomas, S. Bengtson, S.L. Kearns, S.H. Xiao, F. Marone, M. Stampanoni, and P.C.J. Donoghue. 2012a. Distinguishing geology from biology in the Ediacaran Doushantuo biota relaxes constraints on the timing of the origin of bilaterians. *Proceedings of the Royal Society (B: Biological Sciences)* 279: 2369–2376.
- Cunningham, J.A., C.W. Thomas, S. Bengtson, F. Marone, M. Stampanoni, F.R. Turner, J.V. Bailey, R.A. Raff, E.C. Raff, and P.C.J. Donoghue. 2012b. Experimental taphonomy of giant sulphur bacteria: Implications for the interpretation of the embryo-like Ediacaran Doushantuo fossils. *Proceedings of the Royal Society (B: Biological Sciences)* 279: 1857–1864.
- Cunningham, J.A., K. Vargas, Z.J. Yin, S. Bengtson, and P.C.J. Donoghue. 2017. The Weng'an Biota (Doushantuo Formation): an Ediacaran window on soft-bodied and multicellular microorganisms. *Journal of the Geological Society* 174: 793–802.
- Gostling, N.J., C.-W. Thomas, J.M. Greenwood, X.P. Dong, S. Bengtson, E.C. Raff, R.A. Raff, B.M. Degnan, M. Stampanoni, and P.C.J. Donoghue. 2008. Deciphering the fossil record of early bilaterian embryonic development in light of experimental taphonomy. *Evolution and Development* 10: 339–349.
- Hagadorn, J.W., S.H. Xiao, P.C.J. Donoghue, S. Bengtson, N.J. Gostling, M. Pawlowska, E.C. Raff, R.A. Raff, F.R. Turner, C.Y. Yin, C.M. Zhou, X.L. Yuan, M.B. McFeely, M. Stampanoni,

- and K.H. Neelson. 2006. Cellular and subcellular structure of Neoproterozoic animal embryos. *Science* 314: 291–294.
- Huldtgren, T., J.A. Cunningham, C.Y. Yin, M. Stambanoni, F. Marone, P.C.J. Donoghue, and S. Bengtson. 2011. Fossilized nuclei and germination structures identify Ediacaran “animal embryos” as encysting protists. *Science* 334: 1696–1699.
- Pang, K., Q. Tang, J.D. Schiffbauer, J. Yao, X.L. Yuan, B. Wan, L. Chen, Z.J. Ou, and S.H. Xiao. 2013. The nature and origin of nucleus-like intracellular inclusions in Paleoproterozoic eukaryote microfossils. *Geobiology* 11: 499–510.
- Raff, E.C., J.T. Villinski, F.R. Turner, P.C.J. Donoghue, and R.A. Raff. 2006. Experimental taphonomy shows the feasibility of fossil embryos. *Proceedings of the National Academy of Sciences of the United States of America* 103: 5846–5851.
- Raff, E.C., K.L. Schollaert, D.E. Nelson, P.C.J. Donoghue, C.W. Thomas, F.R. Turner, B.D. Stein, X.P. Dong, S. Bengtson, and T. Huldtgren. 2008. Embryo fossilization is a biological process mediated by microbial biofilms. *Proceedings of the National Academy of Sciences of the United States of America* 105: 19360–19365.
- Schiffbauer, J.D., S.H. Xiao, K. Sen Sharma, and G. Wang. 2012. The origin of intracellular structures in Ediacaran metazoan embryos. *Geology* 40: 223–226.
- Sun, W.C., Z.J. Yin, J.A. Cunningham, P. Liu, M. Zhu, and P.C.J. Donoghue. 2020. Nucleus preservation in early Ediacaran Weng’an embryo-like fossils, experimental taphonomy of nuclei and implications for reading the eukaryote fossil record. *Interface Focus* 10: 20200015.
- Xiao, S.H., and A.H. Knoll. 1999. Fossil preservation in the Neoproterozoic Doushantuo phosphorite Lagerstätte, South China. *Lethaia* 32: 219–240.
- Xiao, S.H., and A.H. Knoll. 2000. Phosphatized animal embryos from the Neoproterozoic Doushantuo Formation at Weng’an, Guizhou, South China. *Journal of Paleontology* 74: 767–788.
- Xiao, S.H., Y. Zhang, and A.H. Knoll. 1998. Three-dimensional preservation of algae and animal embryos in a Neoproterozoic phosphorite. *Nature* 391: 553–558.
- Xiao, S.H., J.W. Hagadorn, C.M. Zhou, and X.L. Yuan. 2007a. Rare helical spheroidal fossils from the Doushantuo Lagerstätte: Ediacaran animal embryos come of age? *Geology* 35: 115–118.
- Xiao, S.H., C.M. Zhou, and X.L. Yuan. 2007b. Palaeontology—undressing and redressing Ediacaran embryos. *Nature* 446: E9–E10.
- Xiao, S.H., A.D. Muscente, L. Chen, C.M. Zhou, J.D. Schiffbauer, A.D. Wood, N.F. Polys, and X.L. Yuan. 2014a. The Weng’an biota and the Ediacaran radiation of multicellular eukaryotes. *National Science Review* 1: 498–520.
- Xiao, S.H., C.M. Zhou, P.J. Liu, D. Wang, and X.L. Yuan. 2014b. Phosphatized Acanthomorphic Acritarchs and Related Microfossils from the Ediacaran Doushantuo formation at Weng’an (South China) and their implications for biostratigraphic correlation. *Journal of Paleontology* 88: 1–67.
- Yin, Z.J., and M.Y. Zhu. 2012. New observations of the ornamented Doushantuo embryo fossils from the Ediacaran Weng’an Biota, South China. *Bulletin of Geosciences* 87: 171–181.
- Yin, L.M., M.Y. Zhu, A.H. Knoll, X.L. Yuan, J.M. Zhang, and J. Hu. 2007. Doushantuo embryos preserved inside diapause egg cysts. *Nature* 446: 661–663.
- Yin, Z.J., M.Y. Zhu, P. Tafforeau, J.Y. Chen, P.J. Liu, and G. Li. 2013. Early embryogenesis of potential bilaterian animals with polar lobe formation from the Ediacaran Weng’an Biota, South China. *Precambrian Research* 225: 44–57.
- Yin, Z.J., M.Y. Zhu, D.J. Bottjer, F.C. Zhao, and P. Tafforeau. 2016. Meroblastic cleavage identifies some Ediacaran Doushantuo (China) embryo-like fossils as metazoans. *Geology* 44: 735–738.
- Yin, Z.J., J.A. Cunningham, K. Vargas, S. Bengtson, M.Y. Zhu, and P.C.J. Donoghue. 2017. Nuclei and nucleoli in embryo-like fossils from the Ediacaran Weng’an Biota. *Precambrian Research* 301: 145–151.
- Yin, Z.J., K. Vargas, J.A. Cunningham, S. Bengtson, M.Y. Zhu, F. Marone, and P.C.J. Donoghue. 2019. The early Ediacaran Caveasphaera Foreshadows the evolutionary origin of animal-like embryology. *Current Biology* 29: 4307–4314.
- Yin, Z.J., W.C. Sun, P.J. Liu, M.Y. Zhu, and P.C.J. Donoghue. 2020. Developmental biology of Helicoforamina reveals holozoan affinity, cryptic diversity, and adaptation to heterogeneous environments in the early Ediacaran Weng’an biota (Doushantuo Formation, South China). *Science Advances* 6: eabb0083.
- Zhang, X.G., and B.R. Pratt. 2014. Possible algal origin and life cycle of ediacaran doushantuo microfossils with dextral spiral structure. *Journal of Paleontology* 88: 92–98.